

The molecular nature of superfluidity: Viscosity of helium from quantum stochastic molecular dynamics simulations over real trajectories

Phil Attard

phil.attard1@gmail.com August 31–September 27, 2024

Using quantum equations of motion for interacting bosons, stochastic molecular dynamics simulations with quantized momenta are performed for Lennard-Jones helium-4. The viscosity of the quantum liquid is significantly less than that of the classical liquid, being almost 5 times smaller at the lowest temperature studied. The classical and quantum liquids are identical except for Bose-Einstein condensation, which pinpoints the molecular mechanism for superfluidity. The results rely on the existence of stochastic but real particle trajectories, which has implications for the interpretation of quantum mechanics.

I. INTRODUCTION

Shut up and calculate (1.1)

is an aphorism apparently due to Mermin, although some say Feynman (Mermin 1989, 2004). The sentiment, which is widespread and likely predates the specific phrase, suggests that it is a waste of time to speculate about the interpretation of quantum mechanics since everyone agrees upon the fundamental equations. It acknowledges the spookiness of quantum non-locality and the jittery state of Schrödinger's cat, but it insists that the physical meaning of these has no bearing on the application of the quantum laws and equations, which themselves are unambiguous.

It is certainly true that any theory or calculation is bound by the mathematical rules. Nevertheless I think that it goes too far to say that the physical interpretation of those rules is irrelevant or that the discussion of fundamental quantum concepts is mere sophistry. Once one goes beyond the highly idealized undergraduate textbook examples to work on real world problems, it is necessary to introduce approximations into the fundamental quantum equations. Such approximations may involve neglecting particular classes of terms while resumming others, defining parameters and taking small or large asymptotic limits, choosing specific functions for expansion series, imposing particular boundary conditions, etc. The approach chosen depends not just upon the physical characteristics of the problem at hand but also upon the interpretation of quantum mechanics that leads to an understanding of what is important and what is negligible, what is doable and what is forbidden. It is often the case that the real world application is so far removed from the fundamental quantum equations that the results of an early decision for the research direction cannot be fully anticipated or easily undone. Different interpretations can lead to widely divergent theories due to the sensitivity to the initial beliefs, if you will.

Let me give a concrete example that is directly relevant to the present paper on computing the viscosity of

helium in the superfluid regime. The Copenhagen interpretation of quantum mechanics holds that the world is not objectively real and that it only comes into existence when it is measured or observed. More specifically, particles only possess position or momentum at the time of measurement, and that only one of these can be measured at a time. Therefore, it is said, a particle does not possess simultaneously position and momentum. The corollary of this is that particles cannot follow a path from one position-momentum point to another, which is to say that particle trajectories do not exist.

Obviously any scientist who wishes to understand superfluidity at the molecular level and who believes in the Copenhagen interpretation of quantum mechanics would never consider developing a theory or approximation that is based upon real particles with actual positions and momenta following actual trajectories in time. This example illustrates how a particular interpretation of quantum mechanics can proscribe from the start the theories or approximations that are even considered, let alone explored.

The results in this paper are based on real particles with simultaneously specified positions and momenta, and on real molecular trajectories in time. These obviously contradict the Copenhagen interpretation of quantum mechanics. But do they contradict the equations of quantum mechanics? Obviously I argue not, as I now briefly explain.

It is certainly true that the position and momentum operators do not commute and that Heisenberg's uncertainty principle bounds the product of the variance of the expectation values of the position and momentum operators. These are indisputable mathematical facts. Anything beyond these is a matter of interpretation, and highly questionable interpretation at that. For example, the assertion that an expectation value is a measurement is dubious; there are entire journals devoted to the quantum theory of measurement and the only thing that the various authors agree upon is that a measurement is not simply an expectation value. Further, it is not at all clear that the lack of commutativity of the position and momentum operators implies the Copenhagen interpre-

tation that a particle cannot possess simultaneously a position and a momentum. For a counter-example, see the de Broglie-Bohm pilot wave theory, which reproduces all of the known results of quantum mechanics (Bohm 1952, de Broglie 1928, Goldstein 2024).

The approach used here is predicated on the interpretation that it is the momentum eigenvalue that gives the momentum of a particle, and that a momentum eigenfunction at a particular position should be interpreted as a complex number that is associated with the simultaneous specification of the position and momentum of the particle. In a way that will be made clear, the state of the system is the product of single-particle momentum eigenfunctions of the subsystem, and the subsystem evolves in time by following a trajectory through classical phase space as given by the Schrödinger equation applied to the momentum eigenfunctions and taking into account the interactions with the environment. It is essential to this approach that the subsystem of interest be open and that it can exchange energy and momentum with its environment. (The total system consists of the subsystem and the reservoir or environment.) It is also essential that the symmetrization of the wave function be explicitly accounted for.

At the end of the day, the present interpretation and the consequent approximations that are made should be judged by their physical plausibility and by the results that they produce. One cannot really maintain that the interpretation of quantum mechanics is irrelevant to the real world if the same starting equations combined with different interpretations lead to different quantitative descriptions of that world. The present approach gives a quantitative estimate of the shear viscosity of superfluid helium that includes molecular interactions. Apart from related work by the present author (Attard 2023b, 2025), these are the first such molecular-level results for the superfluid viscosity. It is therefore reasonable to conclude that the proximal impediment to the molecular understanding and quantitative description of superfluidity has been the Copenhagen interpretation of quantum mechanics.

II. ANALYSIS

A. Non-local Dynamics

I have previously given a formally exact formulation of quantum statistical mechanics in classical phase space (Attard 2018, 2021, 2023a). Decoherence due to entanglement with the reservoir or environment is essential to the formulation. In this the configuration picture I rely upon the momentum eigenfunction $\phi_{\mathbf{p}}(\mathbf{q}) = V^{-N/2} e^{-\mathbf{p} \cdot \mathbf{q} / i\hbar}$ (Merzbacher 1970, Messiah 1961). Here for N particles the momentum configuration is $\mathbf{p} = \{\mathbf{p}_1, \mathbf{p}_2, \dots, \mathbf{p}_N\}$, and the position configuration is $\mathbf{q} = \{\mathbf{q}_1, \mathbf{q}_2, \dots, \mathbf{q}_N\}$. The momenta are quantized, with momentum state spacing $\Delta_p = 2\pi\hbar/L$, with $V = L^3$ being

the volume of the cubic subsystem, and $\hbar = 1.05 \times 10^{-34}$ being Planck's constant divided by 2π . The spacing between momentum states goes to zero in the thermodynamic limit. Note that a point in classical phase space, $\mathbf{\Gamma} \equiv \{\mathbf{q}, \mathbf{p}\}$, has the interpretation of a specific configuration of bosons at these positions with these (quantized) momenta, and it has associated with it the complex number $\phi_{\mathbf{p}}(\mathbf{q})$.

For bosons the normalized symmetrized momentum eigenfunction is

$$\phi_{\mathbf{p}}^+(\mathbf{q}) = \frac{1}{\sqrt{N! \chi_{\mathbf{p}}^+}} \sum_{\hat{\mathbf{p}}} \phi_{\hat{\mathbf{p}}\mathbf{p}}(\mathbf{q}), \quad (2.1)$$

$\hat{\mathbf{p}}$ being the permutation operator. The symmetrization factor is

$$\begin{aligned} \chi_{\mathbf{p}}^+ &= \sum_{\hat{\mathbf{p}}} \langle \phi_{\mathbf{p}} | \phi_{\hat{\mathbf{p}}\mathbf{p}} \rangle \\ &= \sum_{\hat{\mathbf{p}}} \delta_{\mathbf{p}, \hat{\mathbf{p}}\mathbf{p}} \\ &= \prod_{\mathbf{a}} N_{\mathbf{a}}(\mathbf{p})!. \end{aligned} \quad (2.2)$$

Here and throughout the occupancy of the single particle momentum state \mathbf{a} is $N_{\mathbf{a}} = \sum_{j=1}^N \delta_{\mathbf{p}_j, \mathbf{a}}$. This is what ultimately drives Bose-Einstein condensation (Attard 2025). The formulation of quantum statistical mechanics relies upon the fact that the subsystem is decoherent due to entanglement with the reservoir or environment.

The Born probability associated with a point in classical phase space for the subsystem in a symmetrized decoherent momentum state is (Attard 2025 Eq. (5.67))

$$\begin{aligned} &\phi_{\mathbf{p}}^+(\mathbf{q})^* \phi_{\mathbf{p}}^+(\mathbf{q}) \\ &= \frac{1}{V^N N! \chi_{\mathbf{p}}^+} \sum_{\hat{\mathbf{p}}', \hat{\mathbf{p}}''} e^{-(\hat{\mathbf{p}}'\mathbf{p} - \hat{\mathbf{p}}''\mathbf{p}) \cdot \mathbf{q} / i\hbar} \\ &\approx \frac{1}{V^N N! \chi_{\mathbf{p}}^+} \sum_{\hat{\mathbf{p}}', \hat{\mathbf{p}}''}^{(\hat{\mathbf{p}}'\mathbf{p} \approx \hat{\mathbf{p}}''\mathbf{p})} e^{-(\hat{\mathbf{p}}'\mathbf{p} - \hat{\mathbf{p}}''\mathbf{p}) \cdot \mathbf{q} / i\hbar}. \end{aligned} \quad (2.3)$$

The reason for neglecting the terms involving permutations of bosons with dissimilar momenta is that these are more or less randomly and uniformly distributed on the unit circle in the complex plane, and so they add up to zero. This is particularly the case when one considers that small changes in the positions may lead to wildly different exponents for any such permutations. The sum that is retained involves only permutations between bosons in the same, or nearly the same, momentum state, in which case the exponent is zero, or close to zero, even for small changes in positions. The number of permutations between bosons in exactly the same momentum states in the double sum is $\sum_{\hat{\mathbf{p}}', \hat{\mathbf{p}}''}^{(\hat{\mathbf{p}}'\mathbf{p} = \hat{\mathbf{p}}''\mathbf{p})} = N! \prod_{\mathbf{a}} N_{\mathbf{a}}(\mathbf{p})! = N! \chi_{\mathbf{p}}^+$. Arguably these are the ones that dominate, with the permutations

between bosons in neighboring momentum states providing a correction.

An open system is decoherent (Attard 2018, 2021, Joos and Zeh 1985, Schlosshauer 2005, Zurek 1991). Decoherence means that the only allowed permutations must satisfy $\hat{P}\mathbf{p} = \mathbf{p}$. Otherwise the symmetrized momentum eigenfunction, $\phi_{\mathbf{p}}^+(\mathbf{q})$, would be a superposition of states.

There is a decoherence time τ_{mix} (Caldeira and Leggett 1983, Schlosshauer 2005, Zurek *et al.* 2003). This likely decreases with increasing distance between permuted momentum states.

Schrödinger's equation for the time evolution of the momentum eigenfunction in a decoherent system for a small time step gives (Attard 2023d, 2025),

$$[\hat{I} + (\tau/i\hbar)\hat{\mathcal{H}}(\mathbf{q})]\phi_{\mathbf{p}}(\mathbf{q}) = \phi_{\bar{\mathbf{p}}}(\bar{\mathbf{q}}). \quad (2.4)$$

Time reversibility and continuity imply that

$$\begin{aligned} \bar{\mathbf{q}}' &= \mathbf{q} + \tau\nabla_{\mathbf{p}}\mathcal{H}(\mathbf{q}, \mathbf{p}), \\ \text{and } \bar{\mathbf{p}}' &= \mathbf{p} - \tau\nabla_{\mathbf{q}}\mathcal{H}(\mathbf{q}, \mathbf{p}). \end{aligned} \quad (2.5)$$

These are Hamilton's classical equations of motion. The second says that a boson's momentum evolves according to the classical force acting on it.

Focussing on the occupied momentum state \mathbf{a} , consecutive permutations of the $N_{\mathbf{a}}$ bosons initially in it has over a time $\tau \gtrsim \tau_{\text{mix}}$ the effect of sharing equally the classical forces acting on them. On average they therefore evolve classically together, each under the influence of identical non-local forces. The dynamics of a momentum state are those of a rigid body, except that the bosons respond to the equally shared non-local forces on an individual stochastic basis (see the next section).

In detail, for short time intervals, $\tau < \tau_{\text{mix}}$, the subsystem can exist in a superposition of permutations of nearby momentum states as each evolves according to local forces. Eventually, however, for $\tau > \tau_{\text{mix}}$ this has to be winnowed down to a small window about a single pure state. This state must satisfy $\hat{P}\bar{\mathbf{p}}'(\tau|\mathbf{q}, \mathbf{p}) = \bar{\mathbf{p}}'(\tau|\mathbf{q}, \mathbf{p})$, for any permutation \hat{P} such that $\hat{P}\mathbf{p} = \mathbf{p}$. This is the state predicted by the non-local force per boson in the initial momentum state. In the random phase analysis of the Born probability above, amongst all the superposed states, the one with the bosons all in the same new momentum state is the one with the greatest weight.

To put it another way, the original momentum configuration with $N_{\mathbf{a}}$ bosons in the momentum state \mathbf{a} evolves along initially $N_{\mathbf{a}}!$ trajectories according to the classical local forces. These trajectories, or the configurations on them, are superposed. Each configuration in the superposition then bifurcates into $N_{\mathbf{a}}!$ further trajectories. Thus the number of superposed trajectories grows exponentially. These trajectories diverge from each other in momentum space, and the most divergent are most quickly culled by the mechanism of decoherence. The trajectories that come to dominate are those that are closest together, which eventually means the one with all the $N_{\mathbf{a}}$ bosons in the same momentum state (cf. Fig. 1). This

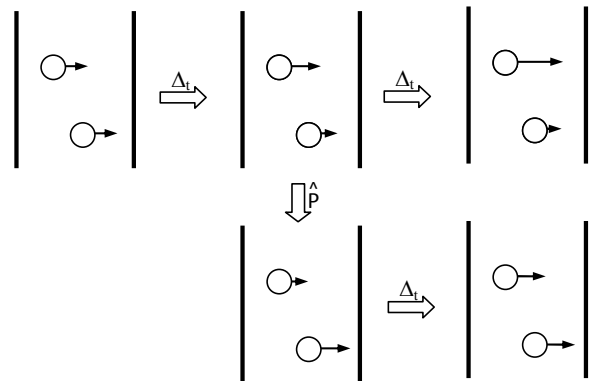


FIG. 1: Two bosons moving near repulsive walls. The bosons are initially in the same momentum state (left). After an intermediate transposition (middle), the final configuration with equal momenta (lower right) has double weight due to its identical transpose. The final configuration with different momenta (upper right) partly cancels with its transpose.

is the trajectory that results from all the bosons sharing equally over the time interval the local forces acting on each of them individually.

Of course from the classical perspective, in the thermodynamic limit the spacing between momentum states becomes infinitesimal, and there is no measurable distinction between the subsystem being in a momentum configuration and being in a superposition of neighboring momentum configurations.

The shared non-local force per boson in momentum state \mathbf{a} is (Attard 2025)

$$\mathbf{F}_{\mathbf{a}} = \frac{1}{N_{\mathbf{a}}} \sum_{j \in \mathbf{a}} \mathbf{f}_j. \quad (2.6)$$

Here the local classical force on boson j is $\mathbf{f}_j = -\nabla_{\mathbf{q},j}U(\mathbf{q})$, where $U(\mathbf{q})$ is the potential energy. The permutation of the momenta of the bosons in a momentum state effectively averages the local forces and applies it non-locally across the momentum state.

The occupation entropy, $S^{\text{occ}}(\mathbf{p}) = k_{\text{B}} \ln \chi_{\mathbf{p}}^+$, acts like an additional force that seeks to keep bosons together in the same momentum state. The shared non-local force preserves the occupation entropy on average.

It should be emphasized that there are two sources of decoherence: there is the internal decoherence that was discussed above on the basis of the Born probability, and there is the eternal decoherence due to the entanglement of the open subsystem with the environment or reservoir. Both mechanisms dictate that the subsystem must be in a pure state where each boson has a position and a momentum. Allowed permutations are between bosons in the same momentum state, and, for limited time periods, also between bosons in neighboring momentum states. Permutations between bosons in different momentum states, which would correspond to the superposition of different momentum configurations, are suppressed, with the sup-

pression increasing with increasing distance between the permuted states.

B. Adiabatic Transition

The change in position of the bosons over a time step τ is deterministic,

$$\mathbf{q}(t + \tau) = \mathbf{q}(t) + \frac{\tau}{m} \mathbf{p}(t). \quad (2.7)$$

The momenta are quantized, with \mathbf{p} being a $3N$ -dimensional vector integer multiple of Δ_p .

Consider the transition of a single boson in the momentum state \mathbf{a} , which has $N_{\mathbf{a}}$ bosons, to a neighboring momentum state \mathbf{a}' , which has $N_{\mathbf{a}'}$ bosons, $\{N_{\mathbf{a}}, N_{\mathbf{a}'}\} \xrightarrow{\tau} \{N_{\mathbf{a}} - 1, N_{\mathbf{a}'} + 1\}$. The conditional transition probability for the time step gives the transition rate. Bayes theorem for the conditional transition probability with microscopic reversibility is (Attard 2012a)

$$\begin{aligned} & \varphi(N_{\mathbf{a}} - 1, N_{\mathbf{a}'} + 1; t + \tau | N_{\mathbf{a}}, N_{\mathbf{a}'}; t) \varphi(N_{\mathbf{a}}, N_{\mathbf{a}'}; t) \\ &= \varphi(N_{-\mathbf{a}}, N_{-\mathbf{a}'}; t | N_{-\mathbf{a}} - 1, N_{-\mathbf{a}'} + 1; t - \tau) \\ & \quad \times \varphi(N_{-\mathbf{a}} - 1, N_{-\mathbf{a}'} + 1; t - \tau), \end{aligned} \quad (2.8)$$

or

$$\begin{aligned} & \frac{\varphi(N_{-\mathbf{a}} - 1, N_{-\mathbf{a}'} + 1; t - \tau)}{\varphi(N_{\mathbf{a}}, N_{\mathbf{a}'}; t)} \\ &= \frac{\varphi(N_{\mathbf{a}} - 1, N_{\mathbf{a}'} + 1; t | N_{\mathbf{a}}, N_{\mathbf{a}'}; t - \tau)}{\varphi(N_{-\mathbf{a}}, N_{-\mathbf{a}'}; t + \tau | N_{-\mathbf{a}} - 1, N_{-\mathbf{a}'} + 1; t)}. \end{aligned} \quad (2.9)$$

If all of the momenta are reversed, $\mathbf{p} \Rightarrow -\mathbf{p}$, then $N_{-\mathbf{a}} = N_{\mathbf{a}}$ and $N_{-\mathbf{a}'} = N_{\mathbf{a}'}$.

The change in potential energy due to the motion of the single boson under consideration during the time step is

$$\begin{aligned} & U(\mathbf{q}(-\mathbf{a}', t - \tau)) - U(\mathbf{q}) \\ &= U(\mathbf{q} + \tau \mathbf{a}'/m) - U(\mathbf{q}) \\ &= \frac{-\tau}{m} \mathbf{F}_{\mathbf{a}} \cdot \mathbf{a}' \\ &= \frac{-\tau}{m} \mathbf{F}_{\mathbf{a}} \cdot \mathbf{a} + \mathcal{O}(\tau \tilde{\Delta}_p). \end{aligned} \quad (2.10)$$

Notice that this takes boson $j \in \mathbf{a}$ to experience the shared non-local force per boson, $\mathbf{F}_{\mathbf{a}} = N_{\mathbf{a}}^{-1} \sum_{k \in \mathbf{a}} \mathbf{f}_k(\mathbf{q})$, rather than \mathbf{f}_j , the local classical force. The total change in potential energy due to bosons in the momentum state \mathbf{a} obtained with the shared non-local force is the same as would have been obtained summing over the change due to the individual local classical forces.

With this, in the occupancy picture (Attard 2021, 2023a, 2025, Pathria 1972), the left hand side of Bayes'

theorem is

$$\begin{aligned} & \frac{\varphi(N_{-\mathbf{a}} - 1, N_{-\mathbf{a}'} + 1; t - \tau)}{\varphi(N_{\mathbf{a}}, N_{\mathbf{a}'}; t)} \\ &= \frac{\varphi(N_{\mathbf{a}} - 1, N_{\mathbf{a}'} + 1; t - \tau)}{\varphi(N_{\mathbf{a}}, N_{\mathbf{a}'}; t)} \\ &= e^{-\beta[a'^2 - a^2]/2m} e^{\beta \tau \mathbf{F}_{\mathbf{a}} \cdot \mathbf{a}/m} \\ &\approx 1 - \frac{\beta}{m} [\mathbf{a}' - \mathbf{a}] \cdot \mathbf{a} + \frac{\beta \tau}{m} \mathbf{F}_{\mathbf{a}} \cdot \mathbf{a} \\ & \quad + \mathcal{O}(\tilde{\Delta}_p^2) + \mathcal{O}(\tau^2) + \mathcal{O}(\tilde{\Delta}_p \tau). \end{aligned} \quad (2.11)$$

This is the occupancy picture and there is no occupation entropy. Most commonly the transition is to the nearest neighbor state, $\tilde{\Delta}_p = \Delta_p$. But as discussed below there may be occasions when it is necessary to jump further afield, in which case $\tilde{\Delta}_p$ is some integer multiple of Δ_p .

For each boson in an occupied state \mathbf{a} , we choose to attempt three successive transitions to a neighbor in the direction of each component of the force, rather than a single transition to one of the seven neighboring states. Also, the shared non-local force per boson $\mathbf{F}_{\mathbf{a}}$ does not change during a time step even though the occupancy of the state may change during a time step as all the bosons in the subsystem sequentially attempt a transition.

For the occupied momentum state \mathbf{a} , the relevant neighbor state in the direction $\alpha \in \{x, y, z\}$ is $\mathbf{a}'_{\alpha} \equiv \mathbf{a} + \text{sign}(\tau F_{\mathbf{a}, \alpha}) \tilde{\Delta}_p \hat{\mathbf{x}}_{\alpha}$. (Most commonly the time step τ is positive and the neighboring momentum state lies in the direction of the force.) The conditional transition probability for the transition $\{N_{\mathbf{a}}, N_{\mathbf{a}'_{\alpha}}\} \xrightarrow{\tau} \{N_{\mathbf{a}} - 1, N_{\mathbf{a}'_{\alpha}} + 1\}$ may be split into even and odd terms,

$$\varphi(N_{\mathbf{a}} - 1, N_{\mathbf{a}'_{\alpha}} + 1; t | N_{\mathbf{a}}, N_{\mathbf{a}'_{\alpha}}; t - \tau) = \varphi_{\alpha}^{+}(\mathbf{a}) + \varphi_{\alpha}^{-}(\mathbf{a}), \quad (2.12)$$

where $\varphi_{\alpha}^{\pm}(-\mathbf{a}) = \pm \varphi_{\alpha}^{\pm}(\mathbf{a})$. The probability of not changing state is $\varphi(N_{\mathbf{a}}, N_{\mathbf{a}'_{\alpha}}; t | N_{\mathbf{a}}, N_{\mathbf{a}'_{\alpha}}; t - \tau) = 1 - \varphi_{\alpha}^{+}(\mathbf{a}) - \varphi_{\alpha}^{-}(\mathbf{a})$. With this and the above result Bayes' theorem reads

$$\begin{aligned} & 1 - \frac{\beta}{m} \text{sign}(\tau F_{\mathbf{a}, \alpha}) \tilde{\Delta}_p a_{\alpha} + \frac{\beta \tau}{m} F_{\mathbf{a}, \alpha} a_{\alpha} \\ &= \frac{\varphi_{\alpha}^{+}(\mathbf{a}) + \varphi_{\alpha}^{-}(\mathbf{a})}{\varphi_{\alpha}^{+}(-\mathbf{a}'_{\alpha}) + \varphi_{\alpha}^{-}(-\mathbf{a}'_{\alpha})} \\ &\approx \frac{\varphi_{\alpha}^{+}(\mathbf{a})}{\varphi_{\alpha}^{+}(\mathbf{a}'_{\alpha})} \left[1 + \frac{\varphi_{\alpha}^{-}(\mathbf{a})}{\varphi_{\alpha}^{+}(\mathbf{a})} + \frac{\varphi_{\alpha}^{-}(\mathbf{a}'_{\alpha})}{\varphi_{\alpha}^{+}(\mathbf{a}'_{\alpha})} \right]. \end{aligned} \quad (2.13)$$

Now assume that to leading order

$$\varphi_{\alpha}^{+}(\mathbf{a}'_{\alpha}) = \varphi_{\alpha}^{+}(\mathbf{a}) [1 + \tilde{\Delta}_p^2 b_{\alpha}], \quad (2.14)$$

and

$$\varphi_{\alpha}^{-}(\mathbf{a}'_{\alpha}) = \varphi_{\alpha}^{-}(\mathbf{a}) = \varphi_{\alpha}^{+}(\mathbf{a}) [\tau c_{\alpha} + \tilde{\Delta}_p d_{\alpha}]. \quad (2.15)$$

These give

$$\begin{aligned} & 1 - \frac{\beta}{m} \text{sign}(F_{\mathbf{a}, \alpha}) \tilde{\Delta}_p a_{\alpha} + \frac{\beta \tau}{m} F_{\mathbf{a}, \alpha} a_{\alpha} \\ &= [1 - \tilde{\Delta}_p^2 b_{\alpha}] \left[1 + 2\tau c_{\alpha} + 2\tilde{\Delta}_p d_{\alpha} \right] \\ &= 1 + 2\tau c_{\alpha} + 2\tilde{\Delta}_p d_{\alpha}, \end{aligned} \quad (2.16)$$

with second order terms neglected. Hence

$$c_\alpha = \frac{\beta}{2m} F_{\mathbf{a},\alpha} a_\alpha, \text{ and } d_\alpha = \frac{\beta}{2m} \text{sign}(\tau F_{\mathbf{a},\alpha}) a_\alpha. \quad (2.17)$$

Both of these are odd in a_α , as required.

The average change in kinetic energy due to the stochastic transition in the α direction is

$$\begin{aligned} \langle \Delta_\alpha \mathcal{K} \rangle &= \frac{\text{sign}(\tau F_{\mathbf{a},\alpha}) \tilde{\Delta}_p a_\alpha}{m} \\ &\quad \times \wp(N_{\mathbf{a}} - 1, N_{\mathbf{a}'_\alpha} + 1; t | N_{\mathbf{a}}, N_{\mathbf{a}'_\alpha}; t - \tau) \\ &= \frac{\text{sign}(\tau F_{\mathbf{a},\alpha}) \tilde{\Delta}_p a_\alpha}{m} [\wp_\alpha^+(\mathbf{a}) + \wp_\alpha^-(\mathbf{a})] \\ &\approx \frac{\text{sign}(\tau F_{\mathbf{a},\alpha}) \tilde{\Delta}_p a_\alpha}{m} \wp_\alpha^+(\mathbf{a}), \end{aligned} \quad (2.18)$$

again to leading order. Since this must equal the negative of the change in potential energy in the α direction, $(\tau/m) F_{\mathbf{a},\alpha} a_\alpha$, we obtain

$$\wp_\alpha^+(\mathbf{a}) = \frac{|\tau F_{\mathbf{a},\alpha}|}{\tilde{\Delta}_p}. \quad (2.19)$$

This must be positive and less than unity, which can be ensured by choosing $\tilde{\Delta}_p = n_\alpha \Delta_p$, where n_α is a positive integer. Choose n_α to be as small as possible, but no smaller. Practical experience with the finite-sized simulations reported below has shown unity to be sufficient, $\tilde{\Delta}_p = \Delta_p$. The smaller the time step the smaller $\wp_\alpha^+(\mathbf{a})$ is and the more likely the boson is to remain in its current momentum state.

Requiring the cancelation of kinetic and potential energies on average ensures energy conservation and the constancy of the equilibrium probability distribution on the stochastic adiabatic trajectory. It means that on average the change in momentum of the bosons in the state is equal to the classical change in momentum due to the force acting on them. Hence we expect that that these stochastic equations of motion will go over to the classical deterministic equations of motion in the thermodynamic limit in the non-condensed regime.

C. Dissipative Transition

The dissipative transitions act like a thermostat and provide a more direct mechanism for the change in occupancy of the momentum states and for the equilibration of the occupancy distribution. For this we first randomly choose a boson from the N bosons in the subsystem, say j . We then choose with probability in inverse proportion to the occupancy of its state whether or not this boson will attempt a transition. (Attempt a transition only if a random number uniformly distributed on the unit interval is less than $1/N_{\mathbf{p}_j}$.) This step is necessary so that all occupied states are treated equally irrespective of their occupancy. Finally, if a transition for j is to be attempted we use the conditional transition probability that follows

for the 27 near neighbor states \mathbf{a}' (including the original state \mathbf{a}). Typically, this sequence of steps is repeated in a block of N . The block is performed typically once every 10 time steps, although less frequent attempts would probably suffice.

The irreversible form of Bayes' theorem is required,

$$\begin{aligned} \frac{\wp(N_{\mathbf{a}'} + 1, N_{\mathbf{a}} - 1 | N_{\mathbf{a}'}, N_{\mathbf{a}})}{\wp(N_{\mathbf{a}'}, N_{\mathbf{a}} | N_{\mathbf{a}'} + 1, N_{\mathbf{a}} - 1)} &= \frac{\wp(N_{\mathbf{a}'} + 1) \wp(N_{\mathbf{a}} - 1)}{\wp(N_{\mathbf{a}'}) \wp(N_{\mathbf{a}})} \\ &= e^{-\beta(a'^2 - a^2)/2m}. \end{aligned} \quad (2.20)$$

There is no time step involved in this. Now $\mathbf{a}' = \mathbf{a} + \mathbf{s} \Delta_p$ and $a'^2 - a^2 = 2\Delta_p \mathbf{s} \cdot \mathbf{a} + \Delta_p^2 s^2$, where $s_\alpha \in \{-1, 0, 1\}$. In view of classical dissipative dynamics based on the second entropy (Attard 2012), the conditional transition probability for $\mathbf{a} \xrightarrow{j} \mathbf{a}'$ has the form

$$\wp(\mathbf{a}' | \mathbf{a}) = \wp_0 + (\mathbf{a}' - \mathbf{a}) \cdot \mathbf{R}_p(\mathbf{a}) / \Delta_p^2. \quad (2.21)$$

Normalization gives $\wp_0 = 1/27$ and

$$\mathbf{R}_p(\mathbf{a}) = \frac{-\Delta_p^2}{54mk_B T} \mathbf{a}. \quad (2.22)$$

It can be confirmed that with this Bayes' theorem is satisfied to quadratic order. This is just the quantized version of the classical drag force.

The heart of the dissipative part of the algorithm is to calculate $\wp(\mathbf{a}' | \mathbf{a})$ for each of the 27 nearest neighbors (including \mathbf{a}), and place these in some one-dimensional order. This divides the unit interval into subintervals of width equal to the respective transition probability. Next choose a random number uniformly distributed on the unit interval. The boson j is moved to the momentum state corresponding to the subinterval into which the random number falls. Obviously if this subinterval corresponds to the original state \mathbf{a} , then no transition is made. The procedure is repeated for a new randomly chosen boson. There is nothing to prevent a boson being chosen more than once in the current block, in which case it could make several transitions, while other bosons have not been chosen at all.

This random choice of N bosons for transition is not essential. It was used for the quantum fluid for the results below. In what is called the classical fluid, all N bosons were cycled through in sequential order for an attempted transition. This difference between the treatment of the two fluids is not expected to be significant. For the quantum fluid a transition was attempted with probability in inverse proportion to the occupancy of its state. For the classical fluid, a transition was always attempted irrespective of the occupancy of its momentum state. This difference is significant.

This quantum dissipative algorithm was tested for ideal bosons. It was found that for $N = 1,000$, $T^* = 0.60$, $\rho^* = 0.80$, it gave the ground state occupancy as $\langle N_{000} \rangle = 22.8(9)$, which can be compared to the exact result 38.9. The results for the excited states were better; for example the first excited state had $\langle N_{001} \rangle = 10.9(2)$

compared to the exact 12.5. For $N = 10,000$ and the same density and temperature, the algorithm gave $\langle N_{000} \rangle = 35.1(38)$, with the exact result in this case being 40.9. The first excited state was $\langle N_{001} \rangle = 26.2(24)$, compared with the exact 27.9. This dependence on system size for the ground state occupancy is acceptable for the present purposes.

1. Alternative Expansion

As an alternative, expand the right hand side as

$$\begin{aligned} & \frac{\wp(N_{\mathbf{a}'} + 1)\wp(N_{\mathbf{a}} - 1)}{\wp(N_{\mathbf{a}'})\wp(N_{\mathbf{a}})} \\ &= e^{-\beta(a'^2 - a^2)/2m} \\ &= 1 - \frac{\beta}{2m}(a'^2 - a^2) + \frac{\beta^2}{8m^2}(a'^2 - a^2)^2 + \mathcal{O}(\Delta_p^3). \end{aligned} \quad (2.23)$$

For the conditional transition probability use the expansion

$$\begin{aligned} & \wp(N_{\mathbf{a}'} + 1, N_{\mathbf{a}} - 1 | N_{\mathbf{a}'}, N_{\mathbf{a}}) \\ &= A(\mathbf{a}) + B(\mathbf{a})(a'^2 - a^2) + C(\mathbf{a})(a'^2 - a^2)^2 + \mathcal{O}(\Delta_p^3). \end{aligned} \quad (2.24)$$

It is straightforward to show that

$$A(\mathbf{a}) = \frac{1}{27} + \mathcal{O}(\Delta_p^2), \text{ and } B(\mathbf{a}) = \frac{-\beta}{108m} + \mathcal{O}(\Delta_p^2). \quad (2.25)$$

The coefficient $C(\mathbf{a})$ can be set to zero and the expansion of the right hand side will remain satisfied at $\mathcal{O}(\Delta_p^2)$.

Results for ideal bosons ($N = 1,000$, $T = 0.60$, $\rho = 0.80$) gave the ground state occupancy as $\langle N_{000} \rangle = 38.0(8)$, compared to the exact 38.9, and the first excited state occupancy as $\langle N_{001} \rangle = 13.3(1)$, compared to the exact 12.5. For $N = 10,000$ the algorithm gave $\langle N_{000} \rangle = 41.9(40)$, compared to the exact 40.9, and $\langle N_{001} \rangle = 28.4(9)$, compared to the exact 27.9.

Although these results for ideal bosons are better than those obtained with the second entropy algorithm, preliminary results suggested that the latter was better for interacting bosons, as judged by the kinetic energy in the classical case. Also the second entropy approach has fundamental justification in the classical limit (Attard 2012a). For these reasons it is the second entropy algorithm that is used to obtain the results given below.

D. Viscosity Time Correlation Function

The shear viscosity can be expressed as an integral of the momentum-moment time-correlation function (Attard 2012a Eq. (9.117)),

$$\eta_{\alpha\gamma}(t) = \frac{1}{2Vk_B T} \int_{-t}^t dt' \left\langle \dot{P}_{\alpha\gamma}^0(\mathbf{\Gamma}) \dot{P}_{\alpha\gamma}^0(\mathbf{\Gamma}(t' | \mathbf{\Gamma}, 0)) \right\rangle. \quad (2.26)$$

It was Onsager (1931) who originally gave the relationship between the transport coefficients and the time correlation functions. It is therefore somewhat puzzling that this is called a Green-Kubo expression (Green 1954, Kubo 1966). The first α -moment of the γ -component of momentum is

$$P_{\alpha\gamma} = \sum_{j=1}^N q_{j,\alpha} p_{j\gamma}. \quad (2.27)$$

The classical adiabatic rate of change of momentum moment is

$$\dot{P}_{\alpha\gamma}^0 = \frac{1}{m} \sum_{j=1}^N p_{j\alpha} p_{j\gamma} + \sum_{j=1}^N q_{j\alpha} f_{j\gamma}. \quad (2.28)$$

This can be shown to be symmetric, $\dot{P}_{\alpha\gamma}^0 = \dot{P}_{\gamma\alpha}^0$.

In the occupancy picture we cannot distinguish individual bosons, and so we should replace here the classical force on individual bosons by the shared non-local force on the bosons in each momentum state. Arguably this is equivalent to using the adiabatic stochastic transition probability since on average the two are the same. Therefore, for the momentum state \mathbf{a} , define the shared non-local force per boson and the center of mass,

$$\mathbf{F}_{\mathbf{a}} \equiv \frac{1}{N_{\mathbf{a}}} \sum_{j \in \mathbf{a}} \mathbf{f}_j, \text{ and } \mathbf{Q}_{\mathbf{a}} \equiv \frac{1}{N_{\mathbf{a}}} \sum_{j \in \mathbf{a}} \mathbf{q}_j. \quad (2.29)$$

Also define the total force on the momentum state \mathbf{a} due to the state \mathbf{b} to be

$$\mathbf{F}_{\mathbf{ab}} = \sum_{j \in \mathbf{a}} \sum_{k \in \mathbf{b}} \mathbf{f}_{jk}, \quad (2.30)$$

where \mathbf{f}_{jk} is the classical force on boson j due to boson k . Note that $\mathbf{F}_{\mathbf{a}} = N_{\mathbf{a}}^{-1} \sum_{\mathbf{b}} \mathbf{F}_{\mathbf{ab}}$. According to Newton, $\mathbf{F}_{\mathbf{ab}} = -\mathbf{F}_{\mathbf{ba}}$ and $\mathbf{F}_{\mathbf{aa}} = \mathbf{0}$. Using these the adiabatic rate of change of the first momentum moment dyadic in the condensed regime is

$$\begin{aligned} \underline{\underline{\dot{P}}}^0 &= \frac{1}{m} \sum_{j=1}^N \mathbf{p}_j \mathbf{p}_j + \sum_{\mathbf{a}} N_{\mathbf{a}} \mathbf{Q}_{\mathbf{a}} \mathbf{F}_{\mathbf{a}} \\ &= \frac{1}{m} \sum_{j=1}^N \mathbf{p}_j \mathbf{p}_j + \sum_{\mathbf{a}} \mathbf{Q}_{\mathbf{a}} \sum_{\mathbf{b}} \mathbf{F}_{\mathbf{ab}} \\ &= \frac{1}{m} \sum_{j=1}^N \mathbf{p}_j \mathbf{p}_j + \frac{1}{2} \sum_{\mathbf{a}, \mathbf{b}} \mathbf{Q}_{\mathbf{ab}} \mathbf{F}_{\mathbf{ab}}, \end{aligned} \quad (2.31)$$

where $\mathbf{Q}_{\mathbf{ab}} = \mathbf{Q}_{\mathbf{a}} - \mathbf{Q}_{\mathbf{b}}$. For the shared non-local force, $\mathbf{f}_j \Rightarrow \mathbf{F}_{\mathbf{p}_j}$, which means that the transformation to the center of mass is exact because all the bosons in the state experience the same force, $\sum_{j \in \mathbf{a}} \mathbf{q}_j \mathbf{f}_j = \sum_{j \in \mathbf{a}} \mathbf{q}_j \mathbf{F}_{\mathbf{a}} = N_{\mathbf{a}} \mathbf{Q}_{\mathbf{a}} \mathbf{F}_{\mathbf{a}}$. In so far as the momentum state is non-local, there are no spatial correlations between the bosons in the state, and on average $\mathbf{Q}_{\mathbf{a}} \approx \mathbf{0}$ (although the fluctuations in this are macroscopic). Similarly the shared

non-local force likely averages close to zero for highly occupied states (again with large fluctuations). These two properties doubtless contribute to the molecular origin of the vanishing of the viscosity for condensed bosons.

Numerical results indicate that this dyadic is symmetric on average, in the same sense that all off-diagonal components of the dyadic are equal on average. The standard deviation of the six off-diagonal components of the viscosity time function gives an estimate of the statistical error.

III. RESULTS

In what follows what is defined as the classical fluid is treated with the same algorithm as the quantum fluid but as if the occupancy of the momentum state was unity. That is, the force on each boson was taken to be the actual local force rather than the shared non-local force, and the dissipative transition was always attempted for the chosen boson irrespective of the occupancy of its momentum state. The viscosity was calculated with the actual local force rather than the shared non-local force. However, the momenta were still quantized and the adiabatic transitions were still stochastic, just as in the quantum case.

We used the Lennard-Jones pair potential,

$$u(r) = 4\epsilon \left[\frac{\sigma^{12}}{r^{12}} - \frac{\sigma^6}{r^6} \right]. \quad (3.1)$$

We set this to zero for $r > 3.5\sigma$. The molecular diameter for helium is $\sigma_{\text{He}} = 0.2556 \text{ nm}$ and the well-depth is $\epsilon_{\text{He}}/k_{\text{B}} = 10.22 \text{ J}$ (van Sciver 2012). The mass is $m_{\text{He}} = 4.003 \times 1.66054 \times 10^{-27} \text{ Kg}$.

The results below are presented in dimensionless form: the temperature is $T^* = k_{\text{B}}T/\epsilon_{\text{He}}$, the number density is $\rho^* = \rho\sigma_{\text{He}}^3$, the time step is $\tau^* = \tau/t_{\text{He}}$, the unit of time is $t_{\text{He}} = \sqrt{m_{\text{He}}\sigma_{\text{He}}^2/\epsilon_{\text{He}}}$, and the shear viscosity is $\eta^* = \eta\sigma_{\text{He}}^3/\epsilon_{\text{He}}t_{\text{He}}$.

A canonical system with $N = 1,000$ Lennard-Jones atoms was simulated with the above quantum stochastic molecular dynamics algorithm. The time step was $\tau^* = 2 \times 10^{-5}$. A block of N dissipative transitions was attempted once every 10 time steps. For the classical liquid this combination consistently gave a kinetic energy 2–3% higher than the exact value. The present parameters were judged acceptable even though a smaller time step or more frequent dissipative transitions would have given more accurate results, albeit at the cost of longer simulation times or greater interference in the adiabatic evolution of the momentum moment. Averages were collected once every 75 time steps. The number of time steps in a run was $10 \times 4,000 \times 75$. A run took about 24 hours on a desk-top personal computer. Four runs were made at each thermodynamic point. The quoted statistical error is the larger of the error estimated from the fluctuations in 10 blocks of each run (averaged across

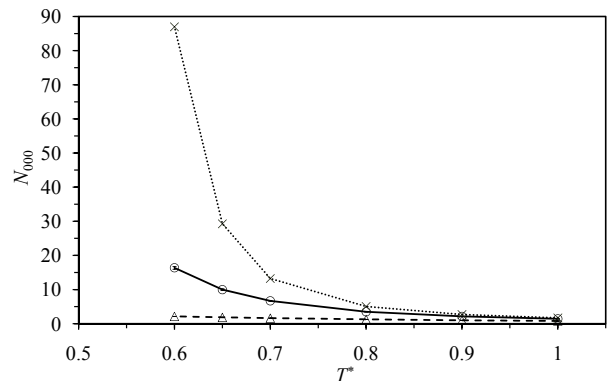


FIG. 2: Ground state occupancy in the saturated Lennard-Jones liquid. The circles are the quantum liquid, the triangles are the classical liquid, and the crosses are the exact result for ideal bosons. The error bars are less than the symbol size. The lines are an eye guide.

the runs), or the standard deviation across the four runs. There was usually little difference in the two estimates (but see below). The shear viscosity time function was estimated for $t^* \leq 6$, which meant that the time correlation function was covered ten times, and that $4 \times 10 \times 6$ values were averaged at each time point for the quantum case, and $4 \times 10 \times 3$ values in the classical case. The components of the quantized momentum were restricted to $p_{j\alpha}^2/2mk_{\text{B}}T \leq 13$.

The liquid saturation curve obtained in previous work was followed (Attard 2023a): $\{T^*, \rho^*\} = \{1.00, 0.7009\}$, $\{0.90, 0.7503\}$, $\{0.80, 0.8023\}$, $\{0.75, 0.8288\}$, $\{0.70, 0.8470\}$, $\{0.65, 0.8678\}$ and $\{0.60, 0.8872\}$.

Figure 2 shows the ground state occupancy on the saturation curve for the Lennard-Jones liquid. It can be seen that the present quantum molecular dynamics algorithm for the quantum liquid gives a larger occupancy than for the classical liquid, but smaller than that for ideal bosons. It has been argued that the ideal boson result should approximately apply to interacting bosons on the far side of the λ -transition (Attard 2025 §5.3). The smaller value evident in the figure could be due to finite size effects, or it could be due to forces in the interacting liquid pushing the ground state to neighboring momentum states, or it could be that the ideal boson model is a poor approximation for interacting bosons.

We defined a quantity `maxocc` to be the occupancy of the maximally occupied momentum state at each instant. For $T^* = 0.65$, `maxocc` = 22.3(2) for the quantum liquid, and 5.5773(4) for the classical liquid. (Here and throughout, the quantity in parentheses is the statistical error for the final digit or digits. It gives the 95% confidence level, as is also the case for the error bars in the figures.) The quantum result is close to the ideal boson result for the ground state occupancy, $N_{000}^{\text{id}} = 29.3$. However, at the higher temperature $T^* = 0.90$, `maxocc` = 9.71(3) in the quantum case, compared to $N_{000}^{\text{id}} = 2.69$. The ground

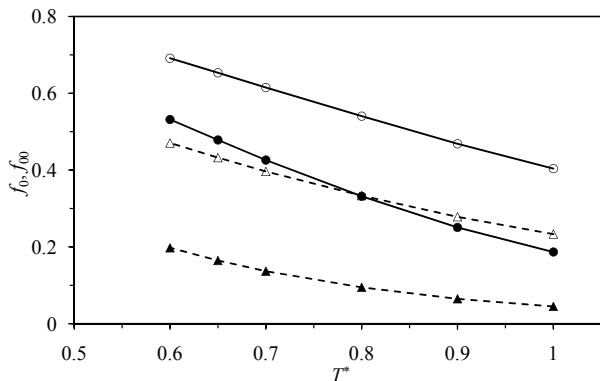


FIG. 3: Fraction of bosons condensed in the saturated Lennard-Jones liquid. The circles are the quantum liquid, the triangles are the classical liquid. The open symbols are f_0 , the fraction in states occupied by two or more bosons, and the filled symbols are f_{00} , the fraction in states occupied by three or more bosons. The error bars are less than the symbol size. The lines are an eye guide.

state occupancy for the quantum liquid, $N_{000}^{\text{qu}} = 2.14(3)$ is not too bad at this temperature.

In any case the occupancy of the ground state is clearly greater for the quantum liquid than for the classical liquid. However, the occupancy of the ground state in the quantum liquid is a small fraction of the total number of bosons in the subsystem. For example, the fraction of the subsystem in the ground state is 1% at $T^* = 0.65$. Obviously this means that ground state condensation cannot account for the λ -transition or for superfluidity.

Figure 3 gives the fraction of condensed bosons in the subsystem. Condensed bosons were defined as those in multiply occupied states, with a threshold set at 2 or 3. In the quantum liquid at the lowest temperature studied about 69% of the bosons are in states with two or more, and about 53% are in states with three or more. In contrast the fraction for the classical liquid is 47% and 20%, respectively. We can conclude that Bose-Einstein condensation is substantial, and that multiple momentum states are multiply occupied. That the majority of the bosons in the system can be considered to be condensed explains the macroscopic nature of the λ -transition and superfluidity.

It can be seen that at higher temperatures the condensation in the quantum liquid is approaching that in the classical liquid, as one would hope. However even at the highest temperature studied, $T^* = 1$, there is still excess condensation in the quantum liquid, $f_0^{\text{qu}} = 40\%$ compared to $f_0^{\text{cl}} = 23\%$. That there remains condensation well-above the superfluid transition temperature is in part due to the neglect in the present calculations of position permutation loops, which suppress condensation (Attard 2025 §3.2). This has implications for the two-fluid model of superfluidity, which is discussed below.

The kinetic energy per boson in the classical liquid is $\beta\mathcal{K}/N = 1.5406(6)$ at $T^* = 0.90$ and $1.5366(3)$ at $T^* =$

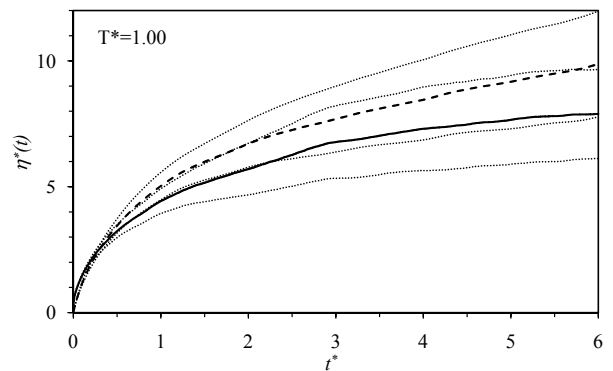


FIG. 4: Shear viscosity time function for the Lennard-Jones liquid at $T^* = 1.00$ and $\rho^* = 0.7009$. The solid curve is the quantum liquid, the dashed curve is the classical liquid, and the dotted curves give the 95% confidence level.

0.60. The equipartition theorem gives the exact classical value as $3/2$. One can conclude that the present stochastic equations of motion that use the transition probability for quantized momentum are indeed going over to the classical equations of motion. The kinetic energy per boson in the quantum liquid is $\beta\mathcal{K}/N = 1.2859(8)$ at $T^* = 0.90$ and $1.001(1)$ at $T^* = 0.60$. The decrease in kinetic energy with decreasing temperature is a manifestation of the increasing condensation in the quantum liquid that preferentially occurs in the low lying momentum states.

Figure 4 shows the shear viscosity time function for the quantum and classical liquids at the relatively high temperature of $T^* = 1.00$. The general features of the curves is that they rise from zero at $t^* = 0$ to reach a maximum or a plateau, in this case at about $t^* = 6$. This maximum value is taken to be ‘the’ shear viscosity. It can be seen that the viscosity of the classical liquid is greater than that of the quantum liquid, although they do agree to within the statistical error over most of the time domain shown. The fraction of condensed bosons in states with two or more bosons at this temperature is 40% for the quantum liquid and 23% for the classical liquid (Fig. 3). Hence although one expects the quantum viscosity to go over to the classical viscosity as the temperature is increased, there still remains substantial Bose-Einstein condensation at this temperature.

The diffusion in the system was relatively small. The root mean square change in separation of a randomly chosen pair of bosons over the course of a run was $0.91(32)$ for the quantum liquid and $0.78(31)$ for the classical liquid. Nevertheless the statistical errors in the average potential energy and pressure were about the same whether estimated within a run or between runs. (Each run was started from an independently equilibrated configuration.) I conclude from this that the subsystem is liquid-like rather than glassy.

Figure 5 gives the shear viscosity time function at the lower temperature of $T^* = 0.80$. Note the change of

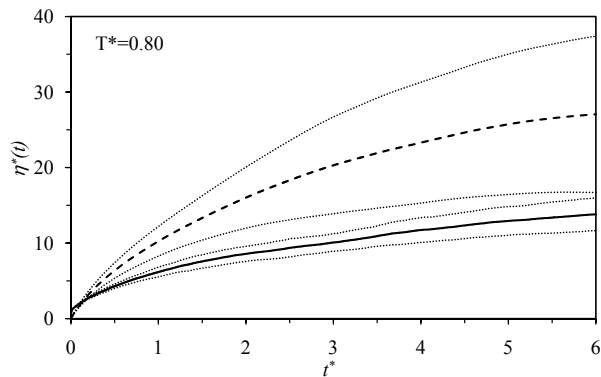


FIG. 5: As in the preceding figure but for $T^* = 0.80$ and $\rho^* = 0.8023$.

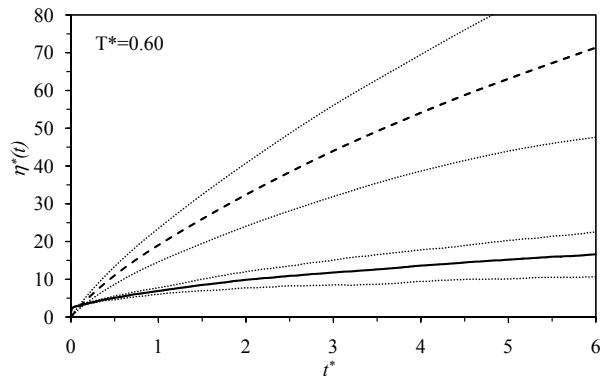


FIG. 6: As in the preceding figure but for $T^* = 0.60$ and $\rho^* = 0.8872$.

scale. The viscosity of the quantum liquid is significantly lower than that of the classical liquid over virtually the whole domain. At very small times the quantum viscosity rises more quickly than the classical viscosity before flattening out. This effect was seen consistently in all the simulations, but the quantitative values in the small time regime appear sensitive to the frequency of the application of the dissipative thermostat (see below). The maximum viscosity of the classical liquid is much greater at this temperature than that at the higher temperature of the preceding figure. The root mean square change in separation was 0.54(16) for the quantum liquid and 0.43(7) for the classical liquid. The statistical errors in the average potential energy and pressure were a little smaller when estimated within a run than when estimated from between runs. I conclude from this that the subsystem is a little glassy.

Figure 5 shows the viscosity for the lowest temperature studied, $T^* = 0.60$. Note the change of scale again. It can be seen that the classical viscosity is substantially larger than the quantum viscosity everywhere except at very short times. The root mean square change in separation was 0.45(14) for the quantum liquid and 0.23(7) for the classical liquid. The statistical errors in the average potential energy and pressure were smaller when estimated

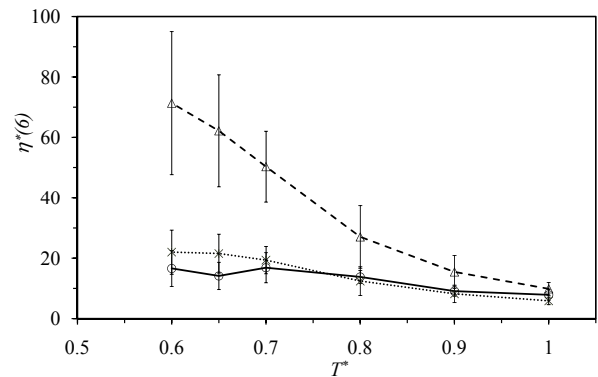


FIG. 7: Shear viscosity at $t^* = 6$ on the Lennard-Jones liquid saturation curve. The circles and solid lines are for the quantum liquid η^{qu} , the triangles and dashed lines are for the classical liquid η^{cl} , and the asterisks and dotted lines are $(1 - f_0^{\text{qu}})\eta^{\text{cl}}$. The error bars give the 95% confidence level, and the lines are an eye guide.

within a run than when estimated from between runs, more noticeably so in the quantum case. I conclude from this that the subsystem is somewhat glassy. If this is the case then it is remarkable that the shear viscosity has a finite value, and that it is so low for the quantum liquid.

The results in this paper are based on the computer algorithm described above. Specifically, that the adiabatic transition for the quantum liquid used the shared non-local force, and that the bosons in each momentum state attempted a transition independently one at a time. An alternative is the so-called rigid body model in which the bosons in a momentum state are tied together so that either all or none make the adiabatic transition each time (Attard 2025). The formula for the shear viscosity is the same in both models. The two models should give the same result on average, but, from the fundamental point of view the present one at a time model is arguably preferable because it allows the adiabatic break-up of an occupied state. For the present case of $T^* = 0.60$ and $\rho^* = 0.8872$, the present shared non-local force one at a time model gives $\eta^*(6) = 16.6(59)$, whereas the rigid body all or nothing model gives $\eta^*(6) = 16.3(75)$.

The present results applied the dissipative block once every 10 time steps, whereas the rigid body results just mentioned applied it once every 5 time steps. Reducing the frequency to once every 25 time steps, (and using runs nearly twice as long) the rigid body model gives $\eta^*(6) = 19.0(28)$. This is unchanged within the statistical error (although the statistical error itself appears smaller for less frequent applications of the dissipative transition). On very short time scales, $t^* \lesssim 0.2$, reducing the frequency of the dissipative transitions causes the viscosity to rise more quickly before flattening out.

Figure 7 shows the shear viscosity at $t^* = 6$ as a function of temperature for the saturated liquid. Based on the extrapolation of fitted quadratics, the viscosity evaluated at this time is relatively close to the maximum

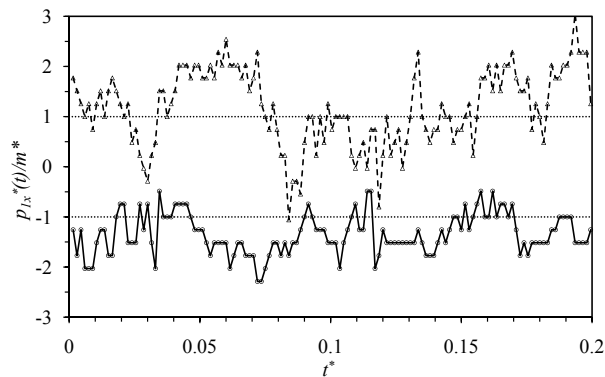


FIG. 8: Component of momentum of a typical boson on a trajectory at $T^* = 0.60$ and $\rho^* = 0.8872$, plotted once every 75 time steps. The circles connected by solid lines are for the quantum liquid (offset by -1) and the triangles connected by dashed lines are for the classical liquid (offset by $+1$). The dotted lines are eye guides and the dimensionless spacing between momentum states is 0.26.

value of the viscosity in almost all cases. It can be seen that at higher temperatures the classical and quantum viscosities converge. At the lowest temperature studied the classical viscosity is about 4.5 times larger than the quantum viscosity. Whereas the classical viscosity increases markedly with decreasing temperature, the quantum viscosity is practically constant. This means that the increase in condensation with decreasing temperature in the quantum liquid, Fig. 3, increases the importance of the shared non-local force, and that this reduces the overall shear viscosity to the extent of overcoming the increasing glassiness of the subsystem.

The figure also includes results for $(1 - f_0^{\text{qu}})\eta^{\text{cl}}(6)$. This viscosity is the analogue of the two-fluid model of superfluidity (Landau 1941, Tisza 1938), namely it is the fraction of uncondensed bosons (ie. those in singly-occupied momentum states) in the quantum liquid times the viscosity in the classical liquid (ie. the viscosity calculated as if all the bosons were in singly-occupied momentum states). We would expect it to have some validity if the viscosity of condensed bosons is zero, and if the actual viscosity is a linear combination of that of the individual components of a two-component mixture. It can be seen that the two-fluid approximation is surprisingly good at lower temperatures. With increasing temperature the quantum and classical viscosities tend toward each other more quickly than the condensation goes to zero. This is the reason that the two-fluid ansatz underestimates the viscosity at the highest temperatures shown.

Of course the virtue of molecular dynamics simulations such as the present is that they enable the classical and quantum viscosities, as well as the distribution of occupancies, to be computed at any thermodynamic state point, and in molecular detail. One wonders how useful the two-fluid model really is, since it does not appear possible to actually measure the individual viscosities or the individual mole fractions in a laboratory.

Figure 8 shows a component of the momentum of a typical boson over time. It can be seen that there is a qualitative difference between the trajectory in the quantum liquid and in the classical liquid. The quantum equations of motion yield a smoother curve, with smaller fluctuations, and noticeable stretches of constant momentum. On this portion of the quantum trajectory, the occupancy of the momentum state that this boson is in ranges up to 26, and averages 5.20. The conclusion is that the shared non-local force in the quantum liquid damps the accelerations experienced by condensed bosons.

IV. CONCLUSION

The two-fluid model of superfluidity (Landau 1941, Tisza 1938) holds that below the λ -transition helium is a mixture of helium I and helium II, with the former having normal viscosity and the latter being the superfluid with zero viscosity. For a bulk measurement, the shear viscosity is believed to be a linear combination of the two in proportion to their mole fraction. Helium II is believed to consist of bosons condensed into the ground energy state.

I say that Bose-Einstein condensation occurs in the low-lying momentum states (Attard 2025). I also say that it is a simplification to divide the liquid into a mixture of two distinct fluids since there are multiple multiply-occupied states. Also, as few as two bosons in the same momentum state experience the effects permutation symmetry. Despite my disdain for the simplicity of the two-fluid model, I must concede that the results in Fig. 7 provide a measure of support for it, at least at low temperatures.

Elsewhere (Attard 2025 §5.3) I have argued that on the far side of the λ -transition ^4He is dominated by momentum loops, which is to say permutations between bosons in the same momentum state. In this case the quantum statistical partition function factorizes into an ideal momentum part and a classical position configuration integral. This predicts that the occupancies of the momentum states are given by ideal statistics, for which the exact analytic results are known (Attard 2025 §2.2, Pathria 1972 §7.1). The present quantum stochastic molecular dynamics results tend to give a smaller occupancy for the ground momentum state, and also for excited momentum states, than that given by ideal statistics. It is possible that this is a finite size effect. Or else it says that interactions play a role in the occupancy and that the proposed factorization (Attard 2025 §5.3) is not entirely accurate. The arguments for the present shared non-local force model relied upon permutations between bosons in neighboring momentum states, not just between those in the same momentum state. In this sense the consequent dynamics are not fully compatible with the factorization model. This matter remains to be clarified.

Although this paper has focussed on the formulation of a computational algorithm for the viscosity of a quan-

tum liquid, it should not be assumed that the molecular equations of motion that are given are merely a numerical technique. The equations of motion yield real trajectories for particles, and there is reason to suppose that expressed in terms of transition probabilities they reflect the underlying reality of nature. This of course has implications for the physical interpretation of quantum mechanics. To which end I suggest

speculate, calculate, and mensurate. (4.1)

References

- Attard P 2012a *Non-equilibrium thermodynamics and statistical mechanics: Foundations and applications* (Oxford: Oxford University Press)
- Attard P 2018 Quantum statistical mechanics in classical phase space. Expressions for the multi-particle density, the average energy, and the virial pressure arXiv:1811.00730
- Attard P 2021 *Quantum Statistical Mechanics in Classical Phase Space* (Bristol: IOP Publishing)
- Attard P 2023a *Entropy beyond the Second Law: Thermodynamics and statistical mechanics for equilibrium, non-equilibrium, classical, and quantum systems* (Bristol: IOP Publishing, 2nd edition)
- Attard P 2023b Quantum stochastic molecular dynamics simulations of the viscosity of superfluid helium arXiv:2306.07538
- Attard P 2023d Hamilton's equations of motion from Schrödinger's equation arXiv:2309.03349
- Attard P 2025 *Understanding Bose-Einstein Condensation, Superfluidity, and High Temperature Superconductivity* (London: Taylor and Francis)
- Bohm D 1952 A suggested interpretation of the quantum theory in terms of hidden variables. I and II. *Phys. Rev.* **85** 166
- de Broglie L 1928 La nouvelle dynamique des quanta, in *Solvay* p. 105
- Caldeira A O and Leggett A J 1983 Quantum tunnelling in a dissipative system *Ann. Phys.* **149** 374
- Goldstein S 2024 Bohmian mechanics *The Stanford Encyclopedia of Philosophy* (Summer 2024 Edition), E N Zalta and U Nodelman (eds.) URL = <https://plato.stanford.edu/archives/sum2024/entries/qm-bohm/>
- Green M S 1954 Markoff random processes and the statistical mechanics of time-dependent phenomena. II. Irreversible processes in fluids. *J. Chem. Phys.* **23**, 298
- Joos E and Zeh H D 1985 The emergence of classical properties through interaction with the environment *Z. Phys. B* **59** 223
- Kubo R 1966 The fluctuation-dissipation theorem *Rep. Prog. Phys.* **29** 255
- Landau L D 1941 Theory of the superfluidity of helium II *Phys. Rev.* **60** 356
- Mermin D 1989 What's wrong with this pillow *Physics Today* **42** 9
- Mermin D 2004 Could Feynman have said this *Physics Today* **57** 10
- Merzbacher E 1970 *Quantum Mechanics* 2nd edn (New York: Wiley)
- Messiah A 1961 *Quantum Mechanics* (Amsterdam: North-Holland volumes 1 and 2)
- Onsager L (1931) Reciprocal relations in irreversible processes. I. *Phys. Rev.* **37** 405. Reciprocal relations in irreversible processes. II. *Phys. Rev.* **38** 2265
- Pathria R K 1972 *Statistical Mechanics* (Oxford: Pergamon Press)
- Schlosshauer M 2005 Decoherence, the measurement problem, and interpretations of quantum mechanics arXiv:quant-ph/0312059v4
- van Sciver S W 2012 *Helium Cryogenics* (New York: Springer 2nd edition)
- Tisza L 1938 Transport phenomena in helium II *Nature* **141** 913
- Zurek W H 1991 Decoherence and the transition from quantum to classical *Phys. Today* **44** 36
- Zurek W H, Cucchietti F M, and Paz J P 2003 Gaussian decoherence from random spin environments arXiv:quant-ph/0312207.